1988

The Beard-Pennock Variable-Stroke Compressor

G. R. Pennock
Purdue University

J. E. Beard
Louisiana State University

THE BEARD-PENNOCK VARIABLE-STROKE COMPRESSOR

G. R. Pennock
School of Mechanical Engineering
Purdue University
West Lafayette, IN 47907.

J. E. Beard
Mechanical Engineering Department
Louisiana State University
Baton Rouge, LA 70803.

ABSTRACT

A new type of variable-stroke compressor, henceforth referred to as the Beard-Pennock compressor, is presented in this paper. The stroke is adjusted by changing the length of the ground link using an auxiliary mechanism. Adjusting the ground link, changes the rotation angle and the effective length of the connecting rod, which in turn controls the pumping volume of the compressor. The pumping action is caused by the motion of the piston which oscillates relative to the frame as the input crank rotates through a complete cycle. The motion of the piston induces a transverse force and a bending moment in the connecting rod but no axial force or static buckling load. Since swirl combustion is known to improve thermal efficiency, the Beard-Pennock variable-stroke compressor was designed to induce high swirl rates. A complete kinematic and dynamic force analysis of the compressor is included in the paper.

INTRODUCTION

Reuleaux, in Chapter IX of his book [6], discusses chamber-crank trains which have been used as engines and pumps. For example, in Article 86, a mechanism is presented which was used as a pump by Bramah and as a steam-engine by both Morgan and Ericsson. The basic mechanism is a crank-rocker four-bar which essentially had a fixed-stroke and compression ratio but could be modified to have an adjustable-stroke and compression ratio. In conventional fixed-stroke internal-combustion engines, the power is controlled by throttling the inlet which impairs the engine efficiency. However, an adjustable-stroke engine has the potential to reduce fuel consumption. Siegla and Siewert [8], for example, reported fuel economy improvements ranging from 2-20 percent, depending upon the frictional losses and the vehicle power-to-weight ratio, for an adjustable-stroke engine over a fixed-stroke engine for particular applications.

The first patents for adjustable-stroke engines and compressors dates back to the end of the last century. Some examples are discussed by Setright [7]. In the design of variable-stroke compressors, Welsh and Riley [9] use a swash plate design to vary the displacement, while Pouliot et al. [5] employ a mechanical linkage which keeps the compression ratio approximately constant. More recently, Freudenstein and Maki [3] made a comprehensive study of thirty-nine variable-stroke mechanisms used for internal-combustion engines. They arrived at an innovative mechanism that changes the stroke while the compression ratio stays almost constant and this mechanism received a patent (U.S. Patent No. 4,270,495; 1981). A variation on a stroke changing mechanism is the AVCR-1360-2 diesel engine [2] where the piston changes height via hydraulics, thereby changing the compression ratio but not the stroke. Although a variable-stroke compressor holds much promise, the problems associated with high surface-to-volume ratio of the combustion chamber at minimum stroke, increased friction, reduced maximum speed, and increased weight have yet to be fully evaluated. A possible application is to use the variable-stroke mechanism, in conjunction with a digital valving system, for a positioning device. For example, the adjustable swash plate pumps presently used for machine tool controls are devices of this type.

In this paper, we present a mechanism with an adjustable-stroke that could be used as a compressor, as a pump, or as an engine [1,5]. For convenience we will refer to the mechanism as the Beard-Pennock variable-stroke compressor, for which a patent is pending. Some of the major advantages associated with the Beard-Pennock variable-stroke compressor are:

1. The compression ratio can be adjusted from a desired finite value to an infinite value.
2. By placing pockets on opposite sides of the piston, the compression and expansion of the gas in the different pockets can take place at the same time.
3. There are no axial forces or static buckling loads acting on the connecting rod.
4. The variable-stroke compressor can be manufactured using standard machine tools.

KINEMATIC ANALYSIS

A schematic diagram of the Beard-Pennock variable-stroke compressor is shown in Fig. 1a. The pumping action is produced by the oscillating motion of the piston (link 4) relative to the frame (link 5) as the input crank (link 2) rotates through a complete cycle. The stroke of the compressor is adjusted by changing the length of the ground link (link 1). This is accomplished by moving the frame along the X-axis by an auxiliary mechanism attached to the frame (not shown in the figure). Moving the frame in the positive X-direction increases the effective length of the connecting rod (link 3) and decreases the amount of rotation of the piston which in turn decreases the compression ratio and the swept volume.

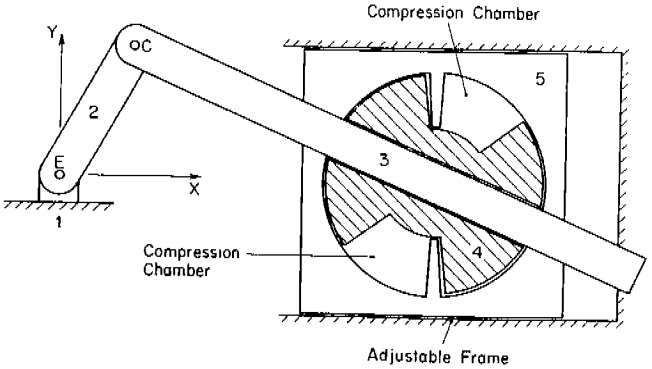

Fig. 1a. Schematic Diagram of The Beard-Pennock Variable-Stroke Compressor.

Two loop-closure equations are required in order to perform a complete kinematic analysis of the variable-stroke compressor, see Fig. 1b, they are:
i) from the main bearing E to the crankpin C, from C to the mass center of the piston G4 (taken to be coincident with the geometric center of the piston), and then from G4 back to E; and ii) from the main bearing E to the crankpin C, from C to the mass center of the connecting rod G3, and then from G3 back to E.

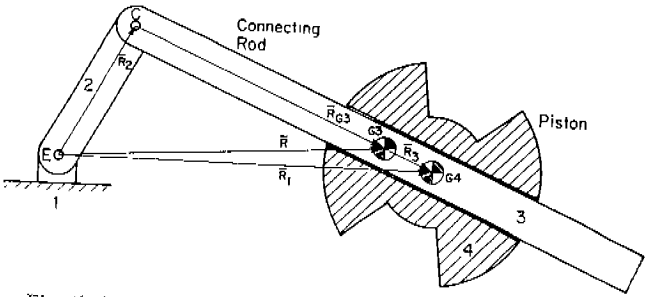

Fig. 1b. Vector Loops for the Variable-Stroke Compressor.

The first loop-closure equation may be written as

$$\bar{R}_2 + \bar{R}_3 - \bar{R}_1 = 0 \tag{1}$$

where $R_1 = E\ G4$ is the length of the adjustable ground link. $R_2 = EC$ is the length of the input crank, and

$$R_3 = C\ G4 = \sqrt{R_1^2 + R_2^2 - 2\ R_1\ R_2 \cos\theta_2} \tag{2}$$

is referred to as the effective length of the connecting rod. The X and Y-components of Eq. (1), respectively, are

$$R_2 \cos\theta_2 + R_3 \cos\theta_3 - R_1 \cos\theta_1 = 0 \quad \text{and} \quad R_2 \sin\theta_2 + R_3 \sin\theta_3 - R_1 \sin\theta_1 = 0 \tag{3}$$

The position of the connecting rod relative to the X-axis, obtained by rearranging Eqs. (3) and dividing, is

$$\theta_3 = \tan^{-1}\left(\frac{\mu_{12} \sin\theta_1 - \sin\theta_2}{\mu_{12} \cos\theta_1 - \cos\theta_2}\right)$$

where $\mu_{ij} = \dfrac{R_i}{R_j}$. The maximum displacement of the piston, measured from the X-axis, occurs when the connecting rod is perpendicular to the input crank, i.e. when

$$(\theta_3)_{max} = \sin^{-1}\mu_{21} \tag{4}$$

and is used to calculate the swept volume of the compressor.

The second loop-closure equation may be written as

$$\bar{R} = \bar{R}_2 + \bar{R}_{G3} \tag{5}$$

where R is the distance from E to G3 and R_{G3} is the distance from C to G3. The X and Y-components of Eq. (5), respectively, are

$$R_X = R_2 \cos\theta_2 + R_{G3} \cos\theta_3 \quad \text{and} \quad R_Y = R_2 \sin\theta_2 + R_{G3} \sin\theta_3 \tag{6}$$

In the velocity and acceleration analysis of the compressor we choose to differentiate the loop-closure equations with respect to the input crank position. We believe that this approach provides insight into the kinematic geometry of the mechanism. The kinematic parameters are a function of only the position of the input crank, i.e. they do not depend upon the state of motion of the crank. The velocity and acceleration analysis is performed for a specified ground link dimension.

The X-component and the Y-component of the acceleration of the mass center of the input crank may be written, respectively, as

$$(a_{G2})_X = (R_{G2})_X\ \omega_2^2 + (R_{G2})_X\ \alpha_2 \quad \text{and} \quad (a_{G2})_Y = (R_{G2})_Y\ \omega_2^2 + (R_{G2})_Y\ \alpha_2 \tag{7}$$

To obtain the acceleration of the mass center of the connecting rod, we adhere to the following procedure. Differentiating Eqs. (3) with respect to the input crank position and writing the results in matrix form gives

$$\begin{bmatrix} \cos\theta_3 & -R_3 \sin\theta_3 \\ \sin\theta_3 & R_3 \cos\theta_3 \end{bmatrix} \begin{bmatrix} f_3 \\ h_3 \end{bmatrix} = \begin{bmatrix} R_2 \sin\theta_2 \\ -R_2 \cos\theta_2 \end{bmatrix} \tag{8}$$

where $f_3 = \dfrac{dR_3}{d\theta_2}$ and $h_3 = \dfrac{d\theta_3}{d\theta_2}$ are referred to as the first-order kinematic coefficients [4] of the connecting rod. The first-order kinematic coefficients, from Eq. (8), are

$$f_3 = R_2 \sin(\theta_2 - \theta_3) \quad \text{and} \quad h_3 = -\mu_{23} \cos(\theta_2 - \theta_3) \tag{9}$$

Differentiating Eqs. (3) twice with respect to the input crank position and writing the results in matrix form gives

$$\begin{bmatrix} \cos\theta_3 & -R_3\sin\theta_3 \\ \sin\theta_3 & R_3\cos\theta_3 \end{bmatrix} \begin{bmatrix} f_3' \\ h_3' \end{bmatrix} = \begin{bmatrix} R_2\cos\theta_2 + 2\,f_3\,h_3\sin\theta_3 + R_3\,h_3^2\cos\theta_3 \\ R_2\sin\theta_2 - 2\,f_3\,h_3\cos\theta_3 + R_3\,h_3^2\sin\theta_3 \end{bmatrix} \tag{10}$$

where $f_3' = \dfrac{d^2R_3}{d\theta_2^2}$ and $h_3' = \dfrac{d^2\theta_3}{d\theta_2^2}$ are the second-order kinematic coefficients of the connecting rod. The second-order kinematic coefficients, from Eq. (10), are

$$f_3' = R_2\cos(\theta_2 - \theta_3) + R_3\,b_3^2 \quad \text{and} \quad h_3' = (1 - 2\,b_3)\,\mu_{23}\sin(\theta_2 - \theta_3) \tag{11}$$

The angular velocity and acceleration of the connecting rod are defined, respectively, as

$$\omega_3 = h_3\omega_2 \quad \text{and} \quad \alpha_3 = h_3\alpha_2 + h_3'\omega_2^2 \tag{12}$$

where the first and second-order kinematic coefficients are as given by Eqs. (9) and (11), respectively. Also, the X and Y-components of the acceleration of the mass center of the connecting rod are defined, respectively, as

$$(a_{G3})_X = (f_{G3})_X\,\alpha_2 + (f_{G3}')_X\,\omega_2^2 \quad \text{and} \quad (a_{G3})_Y = (f_{G3})_Y\,\alpha_2 + (f_{G3}')_Y\,\omega_2^2 \tag{13}$$

where the first and second-order kinematic coefficients, obtained by differentiating Eq. (6) once and twice with respect to the input crank position, resectively, are

$$(f_{G3})_X = -R_2\sin\theta_2 - R_{G3}\,h_3\sin\theta_3 \quad \text{and} \quad (f_{G3})_Y = R_2\cos\theta_2 + R_{G3}\,h_3\cos\theta_3 \tag{14}$$

and

$$(f_{G3}')_X = -R_2\cos\theta_2 - R_{G3}\,h_3^2\cos\theta_3 - R_{G3}\,h_3'\sin\theta_3 \tag{15a}$$

$$(f_{G3}')_Y = -R_2\sin\theta_2 - R_{G3}\,h_3^2\sin\theta_3 + R_{G3}\,h_3'\cos\theta_3 \tag{15b}$$

Plots of the angular position, velocity, and acceleration of the connecting rod versus the position of the input crank are presented in the section entitled "Practical Example and Plots," see Fig. 3. Note that the plots are for steady-state operation of the compressor, i.e. the angular velocity of the input crank is assumed to be constant (the angular acceleration $\alpha_2 = 0$). Since the angular velocity and acceleration of the piston are the same as for the connecting rod this completes the kinematic analysis of the Beard-Pennock variable-stroke compressor. In the following section we present the dynamic force analysis.

DYNAMIC FORCE ANALYSIS

The following assumptions are made in the dynamic force analysis of the Beard-Pennock variable-stroke compressor:

i) The compressor is operating at such a speed that the inertial load exceeds the static load in such great proportions that the static load can be ignored.

ii) The dissipative effects are assumed to be negligible, for example, we neglect friction in the compressor.

iii) The pressure is uniform across each of the piston faces in the compression chamber, i.e. the resultant pressure force acts at the center of the piston face.

iv) The transverse forces exerted by the piston on the connecting rod are analyzed as two resultant forces acting at points A and B, respectively, see Fig. 2b. These forces, which are denoted as $(F_{43})_A$ and $(F_{43})_B$, are assumed to act at the outer radius of the piston, see Fig. 2c.

v) The prototype compressor has four pockets such that face 1 of the piston is parallel to face 3 and face 2 is parallel to face 4, see Fig. 2c. Therefore, the X and Y-components of the resultant forces in the compression chamber cancel. We envisage eight pockets in a future design.

vi) Constant temperature and uniform pressure are assumed in the chamber during compression and expansion. This is a valid assumption especially for an ideal gas (where $PV = nRT$) since the volume decreases uniformly along the faces of the piston.

FORCE AND MOMENT EQUATIONS - Free-body diagrams of the input crank, the connecting rod, and the piston are shown in Figs. 2.

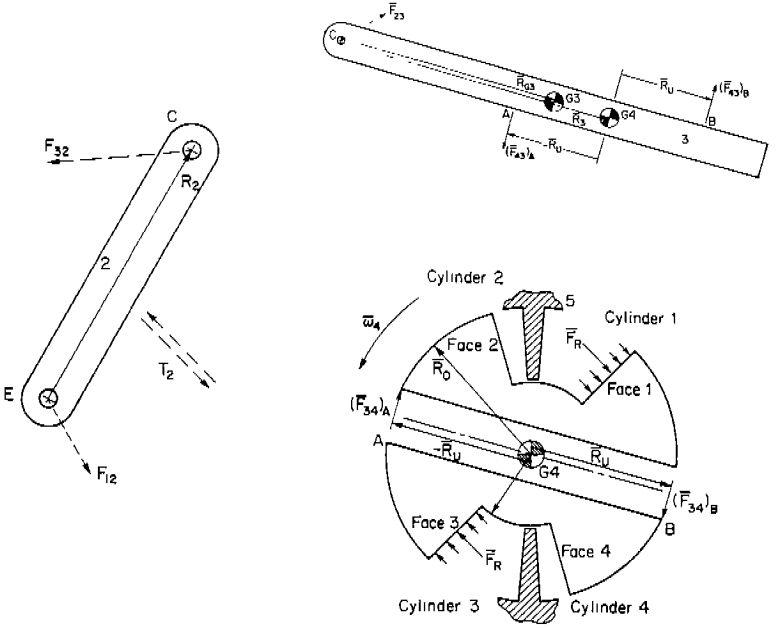

Fig. 2. Free-Body Diagrams.

The X and Y-components of the ground force against the crankshaft may be written, respectively, as

$$(F_{12})_X = -(F_{32})_X + m_2(a_{G2})_X \quad \text{and} \quad (F_{12})_Y = -(F_{32})_Y + m_2(a_{G2})_Y \tag{16}$$

where F_{32} is the force of the connecting rod against the crankpin. The moments about the main bearing E may be written as

$$R_2(\cos\theta_2\,\bar{i} + \sin\theta_2\,\bar{j}) \times [\,(F_{32})_X\,\bar{i} + (F_{32})_Y\,\bar{j}\,] + \bar{T}_2 = I_E\,\bar{\alpha}_2 \tag{17}$$

where T_2 is referred to as the input torque and I_E is the mass moment of inertia of the input crank about the main bearing. For steady-state operation of the compressor, the input torque may be written from Eq. (17) as

$$T_2 = R_2\,[\,(F_{32})_X \sin\theta_2 - (F_{32})_Y \cos\theta_2\,] \tag{18}$$

which is the torque required to maintain a constant angular velocity of the input crank.

The X and Y-components of the force of the crankpin against the connecting rod may be written, respectively, as

$$(F_{23})_X = m_3(a_{G3})_X - [\,(F_{43})_A - (F_{43})_B\,] \sin\theta_3 \tag{19a}$$

$$(F_{23})_Y = m_3(a_{G3})_Y + [\,(F_{43})_A - (F_{43})_B\,] \cos\theta_3 \tag{19b}$$

The moments about the mass center G3 may be written as

$$-R_{G3}\cos\theta_3\,(F_{23})_Y + R_{G3}\sin\theta_3\,(F_{23})_X + (R_{G3} - R_3)\,[\,(F_{43})_A - (F_{43})_B\,] + R_U\,[\,(F_{43})_A + (F_{43})_B\,] = I_{G3}\alpha_3 \tag{20}$$

where R_U is the distance from the mass center G4 to the point of application of the forces $(F_{43})_A$ and $(F_{43})_B$, i.e. the force of the piston against the connecting rod. As stated in assumption (v), these forces are assumed to act at the outer radius of the piston, i.e. $R_U = R_O$. Therefore, substituting Eqs. (19a) and (19b) into Eq. (20) and rearranging gives

$$(R_3 + R_O)(F_{43})_B - (R_3 - R_O)(F_{43})_A = Q \tag{21}$$

where

$$Q = I_{G3}\,\alpha_3 + m_3\,R_{G3}\,[\,(a_{G3})_Y \cos\theta_3 - (a_{G3})_X \sin\theta_3\,] \tag{22}$$

The X and Y-components of the force of the piston against the frame may be written, respectively, as

$$(F_{54})_X = [\,(F_{43})_A - (F_{43})_B\,] \sin\theta_3 \quad \text{and} \quad (F_{54})_Y = -[\,(F_{43})_A - (F_{43})_B\,] \cos\theta_3 \tag{23}$$

The moments about the mass center G4 may be written as

$$R_O\,[\,(F_{43})_A + (F_{43})_B\,] = I_{G4}\,\alpha_4 + 2\,D\,F_R\,R_R \tag{24}$$

where F_R is the resultant pressure force acting on the faces of the piston, R_R is the distance from G4 to the point of application of the force, i.e.

$$R_R = \frac{R_O + R_i}{2} \tag{25}$$

see assumption (iv), and $D = \pm 1$ is referred to as the direction indicator. The direction indicator is negative when the angular velocity of the connecting rod is counterclockwise and positive when the angular velocity is clockwise.

The resultant pressure force acting on the faces of the piston may be obtained from the relation

$$F_R\,R_R = \int_{R_i}^{R_O} P(\theta_2)\,b\,\ell\;d\ell = \frac{b}{2}\,P(\theta_2)\,(R_O^2 - R_i^2) \tag{26}$$

where b and ℓ are the width and length of a piston face, respectively, and $P(\theta_2)$ is the pressure acting on a piston face as a function of the input crank position. Substituting Eq. (26) into Eq. (24) gives

$$R_O\,[\,(F_{43})_A + (F_{43})_B\,] = S \tag{27}$$

where

$$S = I_{G4}\,\alpha_4 + D\,b\,P(\theta_3)\,(R_O^2 - R_i^2) \tag{28}$$

Solving Eqs. (21) and (27) simultaneously, the reaction forces at A and B, respectively, are

$$(F_{43})_A = \frac{S\,(R_3 + R_O) - Q\,R_O}{2\,R_3\,R_O} \quad \text{and} \quad (F_{43})_B = \frac{S\,(R_3 - R_O) + Q\,R_O}{2\,R_3\,R_O} \tag{29}$$

where Q and S are given by Eqs. (22) and (28), respectively. Substituting Eqs. (29) into Eqs. (23), the X and Y-components of the force of the frame against the piston, respectively, are

$$(F_{54})_X = \frac{(S - Q)\sin\theta_3}{R_3} \quad \text{and} \quad (F_{54})_Y = \frac{(Q - S)\cos\theta_3}{R_3} \tag{30}$$

Substituting Eqs. (30) into Eqs. (19a) and (19b), the X and Y-components of the force of the crankpin against the connecting rod, respectively, are

$$(F_{23})_X = m_3(a_{G3})_X + \frac{(Q - S)\sin\theta_3}{R_3} \quad \text{and} \quad (F_{23})_Y = m_3(a_{G3})_Y + \frac{(S - Q)\cos\theta_3}{R_3} \tag{31}$$

Substituting Eqs. (31) into Eqs. (16) and (18) gives the reaction forces $(F_{12})_X$ and $(F_{12})_Y$ and the input torque T_2, respectively. In the following section, the joint reaction forces and the input torque are plotted against the position of the input crank for the prototype Beard-Pennock variable-stroke compressor.

PRACTICAL EXAMPLE AND PLOTS

The link lengths, the masses, and the mass moments of inertia of links 2, 3, and 4 in the prototype Beard-Pennock variable-stroke compressor are presented in Table 1. The width and length of a piston face are, respectively, $b = 5.0$ cms. and $\ell = 5.0$ cms. The outside and inside dimensions of the piston are $R_O = 7.0$ cms. and $R_i = 3.5$ cms., respectively, therefore the location of the resultant pressure force, from Eq. (25), is $R_R = 5.25$cms. The speed of the input crank is assumed to be a constant 1750 R.P.M. counterclockwise.

Table 1. Link Lengths, Masses, and Mass Moments of Inertia.

Links	input crank	connecting rod	piston
link lengths (cms.)	8.5	38.5	see text
mass of links (kgs.)	0.117	1.985	4.690
mass moments of inertia about the mass centers (kgs. cms.^{2})	0.704	214.38	171.92

The pressure in a cylinder is taken to be the same as a comparable slider-crank mechanism. During compression and during expansion the pressure acting on a piston face is determined, respectively, from

$$P(\theta_2) = P_1 \left[\frac{\text{swept volume + clearance volume}}{\text{volume of cylinder}} \right]^{1.3} \quad \text{and} \quad P(\theta_2) = P_2 \left[\frac{\text{clearance volume}}{\text{volume of cylinder}} \right]^{1.3}$$

where the lower and upper limits on the cylinder pressure, respectively, are

$$P_1 = \text{atmospheric} = 1.013 \times 10^5 \text{ Pa} \quad \text{and} \quad P_2 = 10\, P_1$$

The swept volume is calculated from the relation

$$\text{Swept Volume} = 2\, (\theta_3)_{max}\, b\, (R_O^2 - R_i^2)$$

where the maximum displacement of the piston $(\theta_3)_{max}$ is given by Eq. (4).

The following variables are plotted against the input crank position θ_2, for a ground link dimension $R_1 = 17$ cms.: (a) the angular position, velocity, and acceleration of the connecting rod, see Fig. 3.

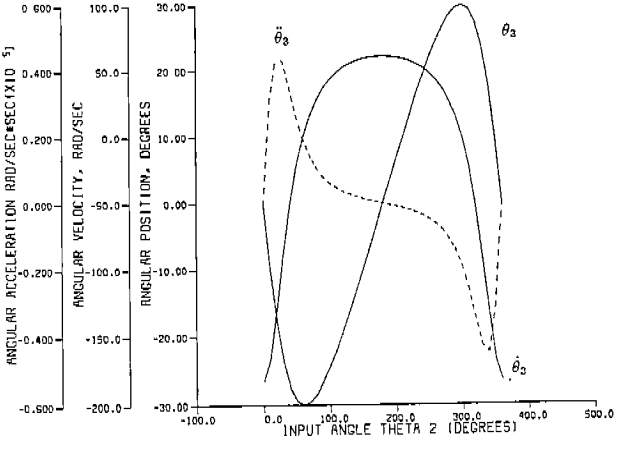

Fig. 3. Angular Position, Velocity, and Acceleration of the Connecting Rod.

(b) the reaction forces $(F_{54})_X$ and $(F_{54})_Y$, see Fig. 4, $(F_{34})_A$ and $(F_{34})_B$, see Fig. 5, and $(F_{12})_X$ and $(F_{12})_Y$, see Fig. 6.

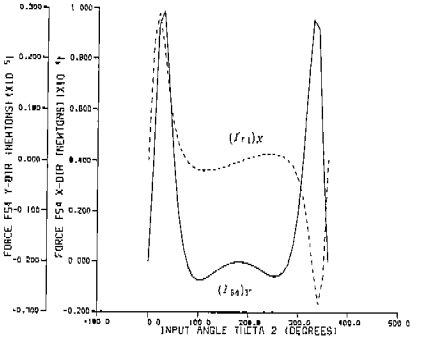

Fig. 4. Reaction Forces $(F_{54})_X$ and $(F_{54})_Y$.

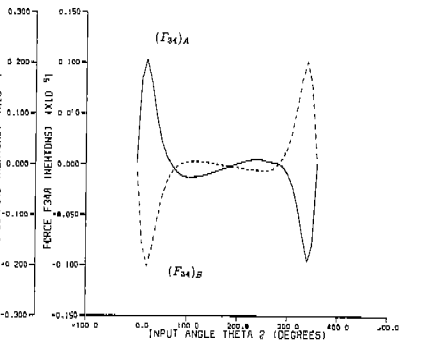

Fig. 5. Reaction Forces $(F_{34})_A$ and $(F_{34})_B$.

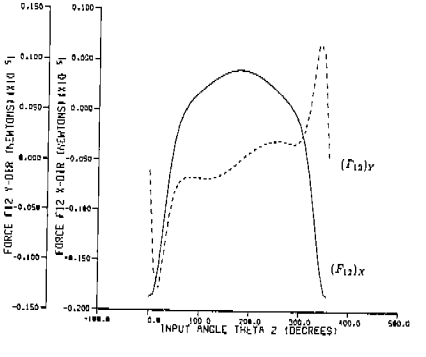

Fig. 6. Reaction Forces $(F_{12})_X$ and $(F_{12})_Y$.

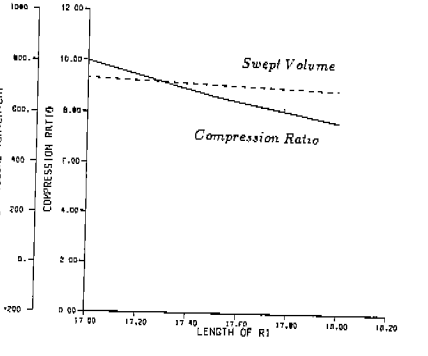

Fig. 7. Swept Volume and Compression Ratio.

Figure 7 shows the swept volume and the compression ratio plotted against the ground link R_1. For purposes of comparison, the input torque is plotted against the position of the input crank for four values of the ground link dimension, namely 17 cms., 19 cms., 21 cms., and 23 cms., see Fig. 8.

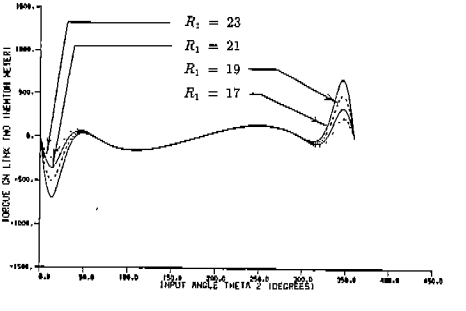

Fig. 8. The Input Torque T_2 against θ_2 for four values of R_1.

CONCLUSION

This paper presents the Beard-Pennock variable-stroke compressor which is of a simple design yet believed to have a practical significance. The change in the swept volume as a function of the piston position approximates a straight line over the entire range of the motion which is desirable in some applications. The change in the compression ratio, as a function of the piston position, is not linear over the entire range. However, it is approximately linear over the second half of the range and this portion can be increased by changing the initial clearance. The input torque required for a constant speed of the input crank has a broad flat range over some 240 degrees of the crank displacement. Since the range is flat for all positions of the piston then this should allow for reasonable requirements on the motor.

An advantage of the Beard-Pennock variable-stroke compressor is that the piston only oscillates, thereby eliminating some of the potential shaking forces. Since the faces of the piston are along the same radial lines. the horizontal and vertical components of the force acting on the frame cancel. By designing the faces of the piston along different radial lines, the effects of the pressure on the frame can be utilized to modify the shaking forces without affecting the torque curve.

REFERENCES

1. Beard, J. E., Hall, A. S., Jr., and Soedel, W., "On The Classification of Compressor, Pump or Engine Designs Using Generalized Linkages," *Proceedings of the 1982 Purdue Compressor Technology Conference,* July 21-23, 1982, pp. 166-172.
2. Ferguson, C. R., *Internal Combustion Engines, Applied Thermosciences,* John Wiley and Sons, 1986, pp. 45-47.
3. Freudenstein, F., and Maki, E. R., "Development of an Optimum Variable Internal-Combustion Engine Mechanism From the Viewpoint of Kinematic Structure," *Journal of Mechanisms, Transmissions, and Automation in Design,* Trans. ASME, Vol. 105, No. 2, June 1983, pp. 259-266.
4. Hall, A. S., Jr., *Mechanism Analysis,* Balt Publishers, Lafayette, Indiana, 1981.
5. Pennock, G.R., and Beard, J.E., "A Variable-Stroke Engine," The International Congress and Exposition, Society of Automotive Engineers, Technical Paper No. 880577, Detroit, Michican, February 29-March 4, 1988.
6. Pouliot, H. N., Delameter, W. R., and Robinson, C. W., "A Variable Displacement Spark-Ignition Engine," International Automotive Engineering, Congress and Exposition, Detroit, SAE Paper No. 770114, February 28-March 4, 1977.
7. Reuleaux, F., *The Kinematics of Machinery,* Macmillan, London, 1963.
8. Setright, L. J. K., *Some Unusual Engines,* Mechanical Engineering Publishing Ltd., I. Mech. E., London, 1975.
9. Siegla, D. C., and Siewert, R. M., "The Variable Stroke Engine - Problems and Promises," Society of Automotive Engineers, West Coast Meeting, San Diego, August 7-10, 1978, Technical Paper Series, Paper No. 780700.
10. Welsh, H. W., and Riley, C. T., "The Variable Displacement Engine: An Advanced Concept Power Plant," Paper 710830, presented at the SAE National Combined Fuels and Lubricants, Powerplant and Truck Meetings, St. Louis, October 26-29, 1971.